

Supporting Information

Multiaxial molecular ferroelectric with record high T_C designed by intermolecular interaction modulation

Jun-Yi Li, Qiu-Ling Xu, Si-Yu Ye, Xiang Chen, Liang Tong, Li-Zhuang Chen*

Table of Content

Experimental section

Fig. S1 Infraed spectrum of compound 4.

Fig. S2 Powder X-ray diffraction (PXRD) of compound 4.

Fig. S3 TG of compound 4.

Fig. S4 DSC curves of compound 4.

Fig. S5 Packing views of compound 1-3.

Fig. S6 Pawly refinement of compound 4.

Fig. S7 PFM measurement of compound 4.

Fig. S8 Topograph pictures of compound 4.

Fig. S9 Crystal morphology of compound 4.

Table S1 T_c of some molecular ferroelectrics.

Table S2 Crystal data of compound 1-4.

Table S3 Polarization calculation

Experimental section

Synthesis

The synthesis of [MeDabco]I salt: The precursor salt was synthesized by pitching methyl iodide into dabco acetonitrile solution with the molar ratio of 1:1 (20mmol:20mmol). After stirring for eight hours at 313 K, vast white sediment can be obtained at the bottom of the flask. All of the product was separated from aqueous phase by reduced pressure distillation and a large amount of sparkling white powder was obtained. The synthesis methods of [FMeDabco]I, [EtDabco]I and [FEtDabco]I salt are same to that of [MeDabco]I except replacing the methyl iodide to fluoromethyl iodide, ethyl iodide and fluoroethyl iodide, respectively. The single crystals of the four compounds can be obtained by slow evaporation of aqueous solutions at room temperature. For **1**, 5 mmol of the [MeDabco]I and zinc iodide were dissolved in 20 mL deionized water, which is also applied in the syntheses of **2-4**. Colourless block crystals can be harvested after three days (Fig. S9). Element analysis calcd (%) for **4**, MW= 605.30, C, 15.87; H, 2.66; N, 4.63; found: C, 15.98; H, 2.86; N, 4.79.

Measurements

PXRD and variable-temperature PXRD measurements were taken on a Rigaku D/MAX 2000 PC X-ray diffraction instrument with CuK α radiation ($\lambda = 1.5405 \text{ \AA}$) in the 2θ range of $5-50^\circ$ with a step size of 0.02° . **IR** spectrum of **4** was measured on a Nicolet iS5 instrument using KBr pellet. **Thermogravimetric analysis (TGA)** was conducted on TGA5500 under nitrogen atmosphere with the ramping rate of 10 K/min. **DSC** for **4** was measured on NETZSCH DSC200F3 instrument under nitrogen atmosphere with

a heating and cooling rate of 15 K/min at the range of 296K-563K.

The single crystal X-ray diffractions for **1-4** were carried out on Bruker Smart Apex CCD II with Mo-K α radiation ($\lambda = 0.71073 \text{ \AA}$). The Apex2 software package was used to process the original data and SHELXLTL-2016 software package was used to solve the crystal structures by the direct methods and refine by full-matrix least-squares refinement. The anisotropically of non-hydrogen atoms were refined for all reflections with $I > 2\sigma(I)$ and the positions of the hydrogen atoms were generated geometrically. Crystallographic data for **1-4** have been deposited at the Cambridge Crystallographic Data Center (CCDC no. 1589848, 2013917, 2013918, 2013919).

P-E hysteresis loop measurement was carried on a Radiant Precision LC II using a typical Sawyer-Tower circuit. The silver glue was painted on the surface of the single crystal, then the crystal was linked with an electrode. The frequency was set as 50 Hz and the E_C is about 7.5 kV/cm.

PFM visualization of the ferroelectric domain structures was carried out using a commercial atomic force microscope system (MFP-3D, Asylum Research). We used conductive Pt/Ir-coated silicon probes (EFM, Nanoworld) to study domain imaging and polarization switching with a resonant-enhanced PFM mode for enhancing the signal.

Hirshfeld surfaces and fingerprint plots

Molecular Hirshfeld surface calculations were performed by using the CrystalExplorer17.5 program with inputting structure file in CIF format. All bond lengths to hydrogen were automatically modified to typical standard neutron values. In this study, all the Hirshfeld surfaces were generated using a standard (high) surface

resolution. The intensity of molecular interaction is mapped onto the Hirshfeld surface by using a red-blue-white color scheme: where the white regions exactly correspond to the distance of Van der Waals contact, the blue ones correspond to longer contacts, and the red ones represent closer contacts.

Table S1 The T_C of some high-temperature molecular ferroelectrics

Compound	T_C /K	Ref.
KH_2PO_4	123	/
PbHPO_4	213	/
$(\text{ABCH})\text{CdCl}_3$	419	[1]
$(4,4\text{-DFHHA})_2\text{PbI}_4$	454	[2]
$[\text{TMAEA}]\text{Pb}_2\text{Cl}_6$	412	[3]
$[(\text{ATHP})_2\text{PbBr}_4]$	503	[4]
<i>R/S</i> -LIPF	483/473.2	[5]
$[\text{3-OQ}]\text{ClO}_4$	457	[6]
$[\text{Hdabco}][\text{ReO}_4]$	499.6	[7]
$[(\text{CH}_3)_3\text{NH}]_3(\text{MnCl}_3)[\text{MnCl}_4]$	481	[8]
$[(\text{AP})\text{RbBr}_3]$	440	[9]
$[\text{FEtDabco}]\text{ZnI}_3$	540	This work

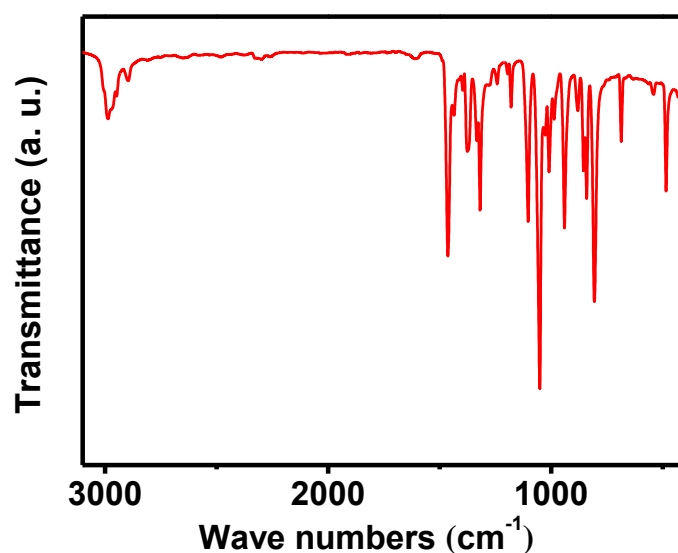


Fig. S1 IR spectrum of compound 4.

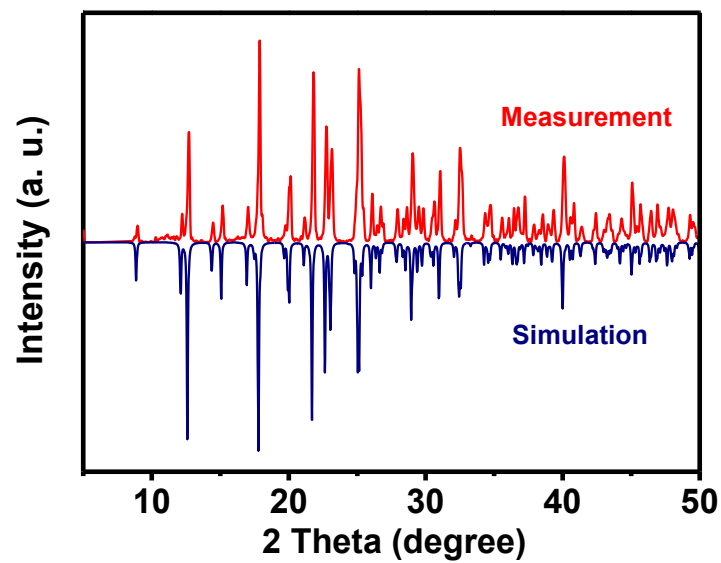


Fig. S2 PXRD pattern of compound **4** at 296K, the red line and the blue line represent measured and simulated result, respectively.

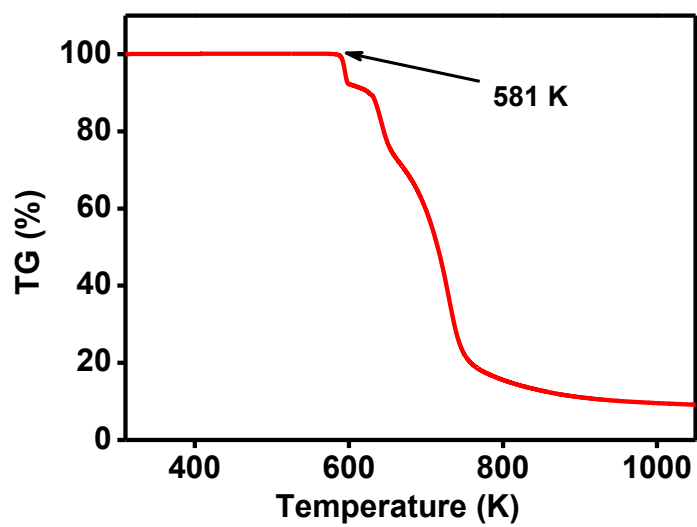


Fig. S3 TG analysis of compound **4**.

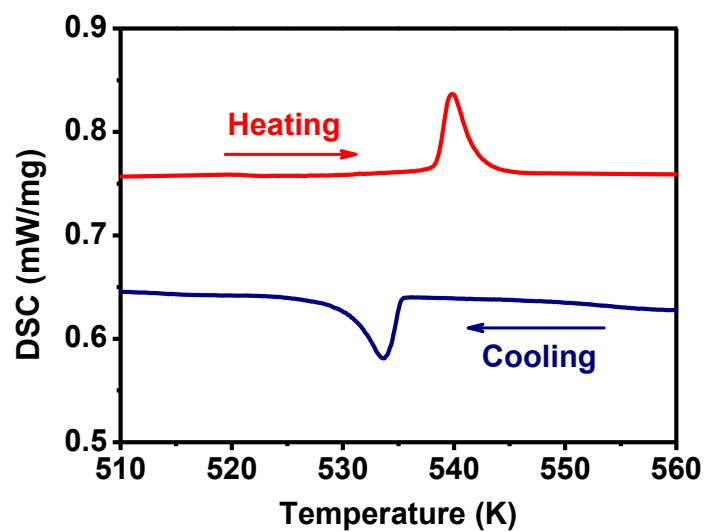


Fig. S4 DSC curves of 4 measured in a heating and cooling run.

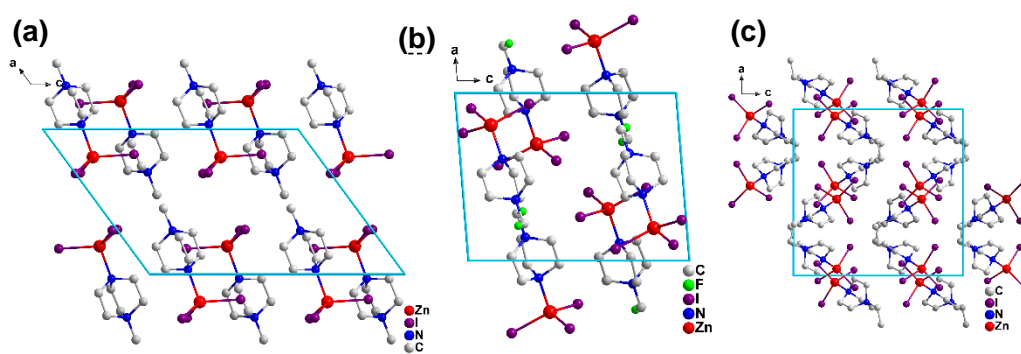


Fig. S5 Packing views of 1 (a), 2 (b) and 3 (c) at 296 K along *b*-axis, all H atoms were omitted for clarify

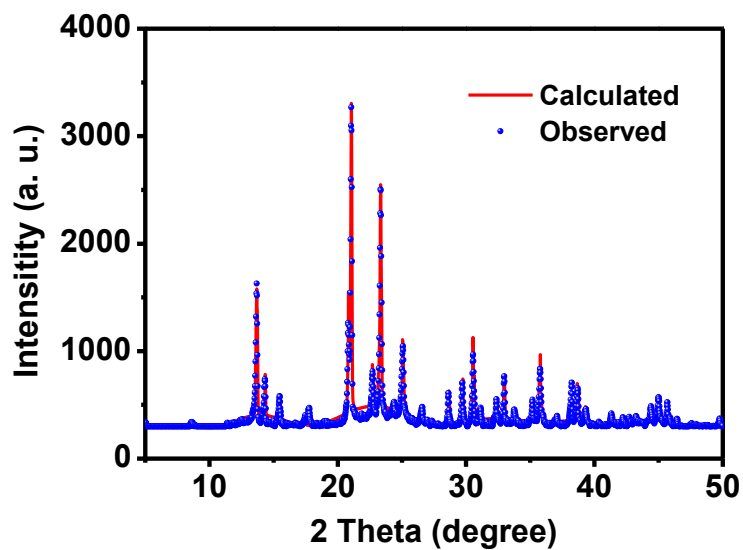


Fig. S6 Pattern of powder X-ray diffraction refined by *Le-Bail* method of **4** at 563 K. The red lines and blue symbol are the calculated and observed profiles, respectively. The refine parameters are $R_p=16.72\%$, $R_{wp}=21.03\%$ and $\chi^2=3.109$.

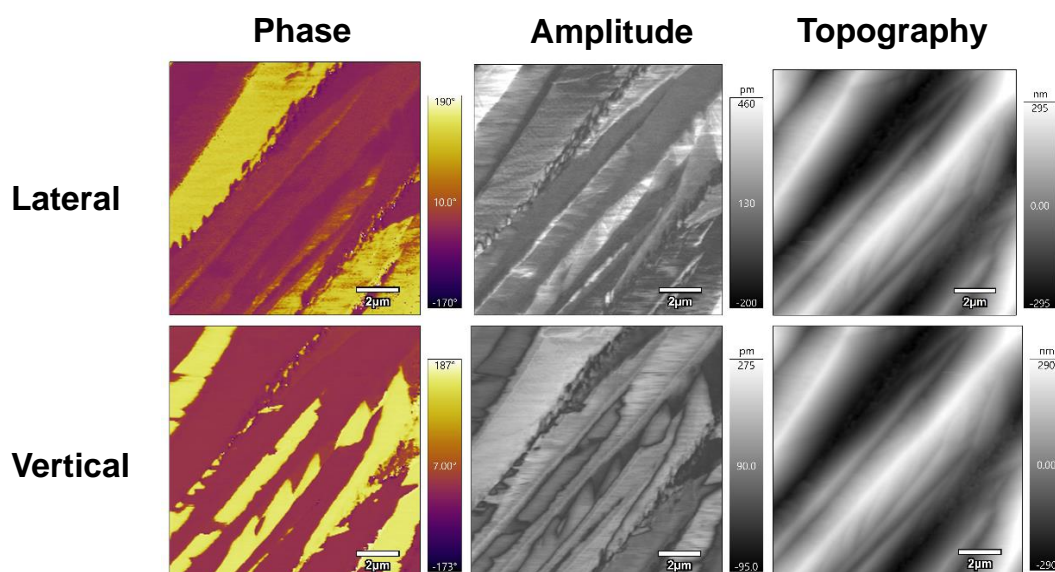


Fig. S7 Lateral (top) and vertical (bottom) PFM phase (left), amplitude (middle) and topography (right) images of the as-grown thin film crystal at another point.

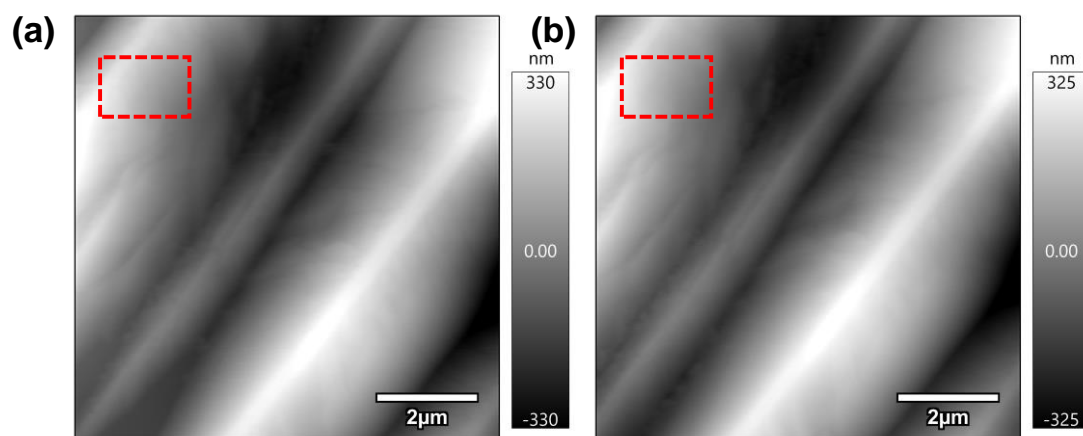


Fig. S8 The lateral (left) and vertical (right) topography of as-grown thin film, both of which in the red dashed box show no obvious distinction with each other, confirming the multi-axial feature.

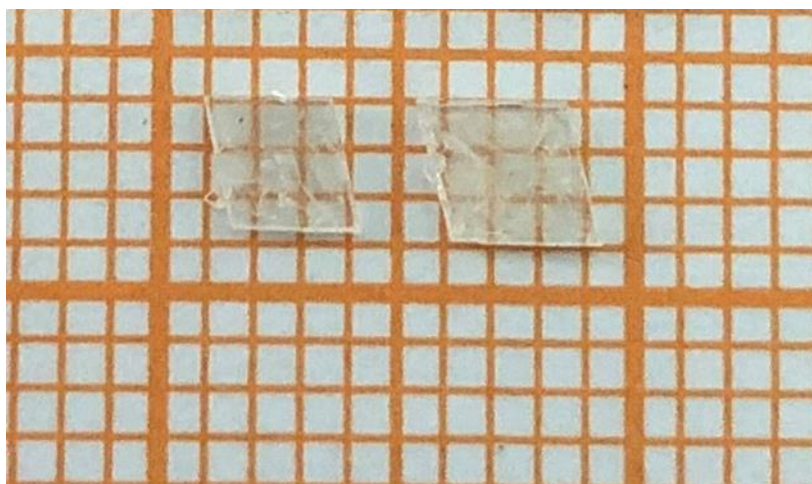


Fig. S9 Crystal morphology of compound **4**.

Table S2 Crystal data and structure refinements for compounds **1-4**

Formula	Zn[Medabco]I ₃	Zn[FMedabco]I ₃	Zn[Etdabco]I ₃	Zn[FEtdabco]I ₃
Formula weight	570.30	591.27	587.30	605.30
Temperature	296 K	296 K	296 K	296 K
Crystal system	Monoclinic	Monoclinic	Orthorhombic	Orthorhombic
Space group	<i>P2₁/c</i>	<i>P2₁/n</i>	<i>Pbca</i>	<i>Pna2₁</i>
<i>a</i> /Å	11.1288(11)	9.5020(3)	14.4585(3)	19.9308(14)
<i>b</i> /Å	9.8748(9)	12.1104(4)	13.1776(3)	7.8474(5)
<i>c</i> /Å	15.7855(14)	12.4906(4)	14.7761(3)	9.8836(7)
<i>α</i> /deg	90	90	90	90
<i>β</i> /deg	126.394(6)	94.573(2)	90	90
<i>γ</i> /deg	90	90	90	90
Volume/Å ³	1396.4(2)	1432.76(8)	2815.27(10)	1545.84(18)
<i>Z</i>	4	4	8	4
Density/g cm ⁻³	2.727	2.741	2.771	2.601
<i>R</i> 1 [<i>I</i> > 2σ(<i>I</i>)]	0.0358	0.0345	0.0577	0.0277
<i>wR</i> 2 [<i>I</i> > 2σ(<i>I</i>)]	0.1103	0.0914	0.1896	0.0728
GOF	1.045	1.122	1.074	1.121

Polarization calculation from point charge analysis

Table S3 Point charge model analysis of [FETDabco]ZnI₃. According to the crystal structure data collected at 296 K, we select a unit cell and assume that the centers of the positive charges and the negative charges are located on the N atom that is bonded with the fluoroethyl and zinc atoms, respectively.

Atoms	Atoms Coordinate	Center Coordinate
Zn	(0.16016, 0.40082, 0.65779)	
	(0.66016, 0.09918, 0.65779)	
	(0.33984, 0.90082, 0.15779)	(0.50000, 0.50000, 0.40779)
	(0.83984, 0.59918, 0.15779)	
N	(0.38818, 0.55902, 0.63920)	
	(0.88818, 0.94098, 0.63920)	(0.50000, 0.50000, 0.38953)
	(0.11182, 0.05902, 0.13920)	
	(0.61182, 0.44098, 0.13920)	

$$\begin{aligned}P_{\text{SIC}} &= \lim \frac{1}{V} \sum q_i r_i \\&= (q_{\text{Mn}} r_{\text{Mn}} + q_{\text{N}} r_{\text{N}}) / V \\&= [(-e \times 0.40779 \times 4) + (e \times 0.38953 \times 8)] \times c / V \\&= -0.01826 \times 1.6 \times 10^{-19} \times 4 \times 9.8836 \times 10^{-10} / (1545.84 \times 10^{-30}) \\&= -0.44719 \mu\text{C cm}^{-2}\end{aligned}$$

Reference

- [1] Y. Y. Tang, Y. F. Xie, Y. L. Zeng, J. C. Liu, W. H. He, X. Q. Huang, R. G. Xiong, *Advanced materials*, 7.
- [2] X. G. Chen, X. J. Song, Z. X. Zhang, H. Y. Zhang, Q. Pan, J. Yao, Y. M. You, R. G. Xiong, *Journal of the American Chemical Society* **2020**, *142*, 10212-10218.
- [3] H. Y. Zhang, X. J. Song, H. Cheng, Y. L. Zeng, Y. Zhang, P. F. Li, W. Q. Liao, R. G. Xiong, *Journal of the American Chemical Society* **2020**, *142*, 4604-4608.
- [4] X. G. Chen, X. J. Song, Z. X. Zhang, P. F. Li, J. Z. Ge, Y. Y. Tang, J. X. Gao, W. Y. Zhang, D. W. Fu, Y. M. You, R. G. Xiong, *Journal of the American Chemical Society* **2020**, *142*, 1077-1082.
- [5] C. K. Yang, W. N. Chen, Y. T. Ding, J. Wang, Y. Rao, W. Q. Liao, Y. Y. Tang, P. F. Li, Z. X. Wang, R. G. Xiong, *Advanced materials* **2019**, *31*, 7.
- [6] C. K. Yang, W. N. Chen, Y. T. Ding, J. Wang, Y. Rao, W. Q. Liao, Y. F. Xie, W. N. Zou, R. G. Xiong, *Journal of the American Chemical Society* **2019**, *141*, 1781-1787.
- [7] Y. Y. Tang, P. F. Li, W. Y. Zhang, H. Y. Ye, Y. M. You, R. G. Xiong, *Journal of the American Chemical Society* **2017**, *139*, 13903-13908.
- [8] P. F. Li, Y. Y. Tang, W. Q. Liao, P. P. Shi, X. N. Hua, Y. Zhang, Z. H. Wei, H. Cai, R. G. Xiong, *Angew. Chem.-Int. Edit.* **2018**, *57*, 11939-11942.
- [9] Q. Pan, Z. B. Liu, Y. Y. Tang, P. F. Li, R. W. Ma, R. Y. Wei, Y. Zhang, Y. M. You, H. Y. Ye, R. G. Xiong, *Journal of the American Chemical Society* **2017**, *139*, 3954-3957.